Section 2: Climate and Water

Contributing Authors: Vinod Mahat and Axel Anderson

2.1 Introduction

The eastern slopes of the Rocky Mountains in Alberta, Canada have highest regional precipitation and the highest runoff ratios (annual streamflow as a proportion of annual precipitation) which generates the majority of streamflow for many rivers including the Oldman River that provides water for domestic and recreational purposes and supports broad base of regional agriculture and fisheries industries in Southern Alberta (Bladon et al., 2008; Emelko et al., 2011; Silins et al., 2009; Stone et al., 2001). Hydrology of Mountainous regions are most likely to be affected by the climate change as precipitation would change from snow to rain in warming climate (IPCC, 2007). Headwater streams and rivers supporting the Oldman River system originates as snow in the eastern slopes of Rocky Mountain and thus are vulnerable to warming climate. Forest change may compound the impacts with the climate change. Given the present near full allocation of water for human use in this region along with the possibility of longer-term limitations in water supply, understanding and predicting how climate and forest changes in this region are likely to affect the production/timing of streamflow are increasingly important (Silins et al., 2009).

There have been numbers of studies into the potential effects of climate change on hydrology and water resources in many regions. Apparent trends in streamflow due to climate change are both increasing and decreasing (Arnell, 1999; Zheng et al., 2009). Arnell (1999) investigated the climate change impacts on water supply on the global scale and reported up to 15% decrease in streamflow in major river basins in year 2050. Studies carried out in different

regions in North America, i.e., Jha et al. (2004) (Upper Mississippi River Basin, USA), Stone et al. (2001) (Missouri River Basin, USA), Hamlet and Lettenmaier (1999) (Columbia River Basin, USA), Kienzle et al. (2012) (North Saskatchewan River basin, AB, Canada) and Stahl et al. (2008) (Bridge River basin, BC, Canada) have reported the streamflow up to 80% increase in fall and winter and 10 to 20% decrease in summer. Barnett et al. (2005) studied the various large basins in the globe and reported streamflow regime in snowmelt-dominated river basins is most sensitive. As melting of winter snow occurs earlier in spring due to temperature rise, there is likely to be future water scarcity in the snow melt dominated regions during the summer. Other studies (e. g. Barnett et al., 2008; Hidalgo et al., 2009; Mote, 2003; Pierce et al., 2008) that are focused on the snowmelt dominated regions have also reported a reduction in snow and early shift in the timing of the streamflow.

GCMs (General Circulation Models or Global Climate Models) are widely used to project future climates under assumed greenhouse gas emission scenarios, both in space and time (e.g. IPCC, 2007; Mehrotra and Sharma, 2010). However, the projections from these models are typically provided at coarse resolutions, i.e. 200 km or more in space and monthly time periods (Wang et al., 2011). The hydrologic processes of interest normally occur at scales on the order of tens to thousands of square kilometers; so the resulting climate projections from GCMs cannot be directly used as input for models at the resolution of interest to hydrologists (Epstein and Ramírez, 1994; Morrison et al., 2002). Consequently, various downscaling techniques that include stochastic, statistical, or dynamic downscaling (Fowler et al., 2007; Maurer et al., 2009; Wang et al., 2011) have been developed to derive higher resolution climate data from the coarser resolution climate projections. Dynamic downscaling refers to the use of regional

climate models (RCMs) (Fowler et al., 2007; Mehrotra and Sharma, 2010). Catchment scale hydrological climate change impact studies have used dynamically downscaled output (e.g. Fowler and Kilsby, 2007; Wood et al., 2004), simple statistical approaches such as multiple regression relationships (e.g. Jasper et al., 2004; Wilby et al., 2000), and stochastic weather generator (e.g. Evans and Schreider, 2002).

Potential impacts of future climate change on hydrology have been assessed through the application of hydrological models driven by the downscaled GCM derived future climates (Campbell et al., 2011; Forbes et al., 2011; Kienzle et al., 2012; Loukas et al., 2002; Toth et al., 2006). A detailed, physically based model could be an effective tool; however, applying detailed model may require large numbers of forcing which are seldom available especially in the mountain regions studies. So, the selection of the model may depend on the availability data for the study region.

The purpose of this study is to evaluate the effects of potential future climate and forest changes on the high water yielding headwaters of Alberta's eastern slopes, focusing on southern portions that supply the overwhelming majority of useable surface water for communities. These Mountain regions are more susceptible to future temperature change as large fraction of the precipitation falling in the regions is snow which partly changes into rain in warming climate affecting the timing and magnitude of streamflow (Forbes et al., 2011; Kienzle et al., 2012). In this study, we include high mountains and examine the possible compounding impacts of forest change.

2.2 Materials and Methods

2.2.1 Study Watershed and Data

The Crowsnest Creek watershed (Figure 2.1), centered at 49.64˚ N, 114.55˚ W, is an important watershed in Southern Alberta, Canada feeding Oldman River which is closed to the issuing of new water extraction licenses due to a growing imbalance between demand and supply [Emelko et al., 2011]. This watershed has a drainage area of 384 km2 with the elevation ranges from 1236 to 2732 m. The watershed is broadly characteristic of Rocky Mountain front-range physiographic settings. Vegetation in the watershed is characterized by Lodgepole pine (Pinus contorta Dougl.ex Loud. Var. latifolia Engelm.) dominated forest at lower elevations, subalpine forest at mid elevations dominated by Engelmann spruce (Picea engelmannii Parry ex Englem.) and subalpile fir (Abies lasiocarpa [Hook.] Nutt.) with alpine ecozones at higher elevations characterized by alpine meadow vegetation and bare rock extending above tree line [Silins et al., 2009].

The majority of the total annual precipitation (50 to 70%) falls as snow from October to April in these catchments. Streamflows in the study area are characteristic of very high water yielding Rocky Mountain streams. Spring snowmelt generally produces the highest continuous streamflows. Rain-on-snow or mid-winter melt events are a common occurrence, producing some of the larger flows, with mean daily discharge in excess of 30 mm day-1. The late summer and over winter period are generally near 0.5–2 mm day-1 (Silins et al., 2009). Hydrology of all these catchments are snowmelt dominated and peak flows are driven by spring snowmelt or rain on spring snowmelt.

Although climate has been monitored continuously with seven climate stations within this watershed by Environment Canada (http://climate.weatheroffice.gc.ca/climateData/canada_e.html), long record of climate data (i.e., about 32 years, from 1965 to 1997) is available only at Coleman climate station which lies approximately at the center of the watershed (Figure 1). We use climate data recorded at this station to drive the daily climatological condition across the entire watershed, here in called the Coleman climate station. Streamflow data used in this study are the data recorded at gauging station, Crowsnest River at Frank (Hydat Station: 05AA008) located close to the city of Blairmore, AB. This station is well suited for the analysis as long-term records of streamflow data, which are necessary for calibrating and validating the model that simulates the effect of climate change on streamflow, are available at this station.

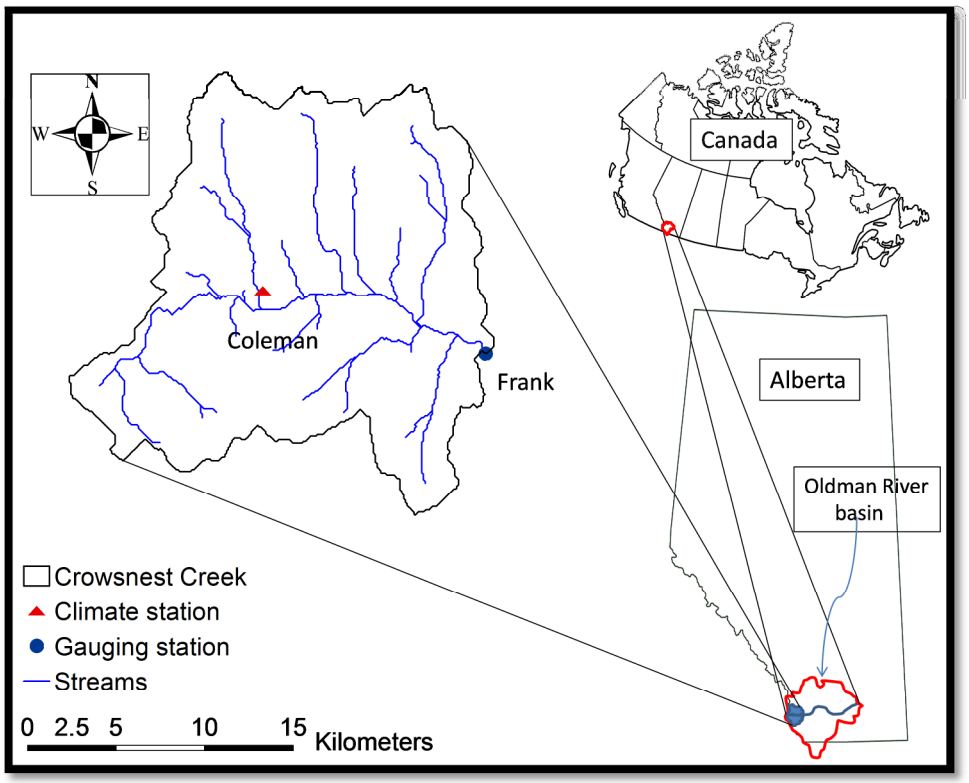

Figure 2.1 Crowsnest Creek watershed with climate station, Coleman and gauging station, Crowsnest at Frank.

2.2.2 Methodology

The study methodology to assess the climate change impacts on streamflow is done in three steps:

- Develop estimates of future monthly climate means (precipitation, maximum temperature Tmax, and minimum temperature, Tmin) in relation to observed (reference) climates at the Coleman climate station,
- Disaggregate (temporal downscale) monthly climate means into daily realizations for use with hydrological model.
- Hydrological model calibration, application and parameter uncertainty.

Estimates of future monthly climate means

Projected monthly climate means used in this study are GCM outputs that are downscaled to 1x1 km grids using climateWNA model (Wang et al., 2006; Wang et al., 2011). ClimateWNA uses a combination of bilinear interpolation and elevation adjustment to downscale the climate data. GCM used in this study is Canadian Climate Center's Modeling and analysis (CCCma) third generation coupled global climate model (CGCM3) (http://www.ec.gc.ca/ccmac-cccma/default.asp?lang=En&n=4A642EDE-1). ClimateWNA downscaled 1x1 km grids from within the study watershed boundary are averaged to estimate the watershed averaged monthly climate means for reference and future periods, and changes in monthly climate means, (i.e., change in mean monthly daily maximum temperature, ΔTmax, change in mean monthly daily minimum temperature, ΔTmin and change in monthly precipitation, ΔP) are calculated as:

〖ΔT〗_max=(〖T_max〗^F+ε)-(〖T_max〗^R+ε) (1)

〖ΔT〗_min=(〖T_min〗^F+ε)-(〖T_min〗^R+ε) (2)

ΔP= 〖ε P〗^F/〖ε P〗^FR (3)

where, TmaxR, TminR and PR are watershed averaged mean monthly daily maximum temperature, mean monthly daily minimum temperature and monthly precipitation, respectively for the reference period, and TmaxF, TminF and PF are watershed averaged mean monthly daily maximum temperature, mean monthly daily minimum temperature and monthly precipitation, respectively for the future period. ε is the bias.

Reference period used in this study is the period between 1965 and 1997, chosen because of the observed daily climates available for the hydrological model calibration and validation during this period. Future periods selected are anomalies for 30-year normal periods 2011–40 (2020s), 2041–70 (2050s), and 2071–2100 (2080s). Three emission scenarios (A1B, A2, and B1) that are developed utilizing the intergovernmental Panel on Climate Change (IPCC) Fourth Assessment Report, AR4 are used. A1B scenario describes "a future world of very rapid economic growth, global population that peaks in mid-century and declines thereafter, and rapid introduction of new and more efficient technologies". A2 scenario describes " economic development is primarily regionally oriented and per capita economic growth and technological change are more fragmented and slower compared to A1B and B1 scenarios; and B1 scenario describes "a convergent world with the same global population that peaks in mid-century and declines thereafter, as in the A1 storyline, but with rapid changes in economic structures toward a service and information economy, with reductions in material intensity, and the introduction of clean and resource-efficient technologies" (IPCC, 2007).

We assume the relative changes in monthly climate means at the Coleman climate station is equivalent to the changes in watershed averaged monthly climate means, ΔTmax, ΔTmin and ΔP that are obtained from equations (1), (2) and (3). Daily observed climate at Coleman is aggregated to monthly scale and perturbed with these ΔTmax, ΔTmin and ΔP to give future monthly climate means at the Coleman climate Station.

Disaggregation

A weather generator can be used to disaggregate monthly climate means into daily realizations for use with hydrological model [Richardson and Wright, 1984]. Weather generators are stochastic numeric models that simulate daily weather data at a single site using the separate statistical properties for each month observed daily weather data for the given site (Racsko et al., 1991; Richardson et al., 1998; Semenov and Brooks, 1999). There are two types of daily weather generators used to determine wet or dry days and precipitation amount. Wet days are days with precipitation larger than zero. The first type, the Markov chain approach, uses a two state first order Markov chain to generate wet or dry day using a random process conditional upon the state of the previous day (Hughes et al., 1999). If a day is determined as wet, then the precipitation amount is computed using two-parameter gamma distribution. The second type, spell-length approach, generates wet or dry series; length of each series is chosen randomly from the wet and dry semi-empirical distribution for the month in which the series starts (Racsko et al., 1991; Wilks, 2012). The wet day precipitation value is generated using semi-empirical precipitation distribution independent of the length of the wet series or the amount of precipitation on previous days (Semenov and Brooks, 1999).

We use Long Ashton Research Station Weather Generator (LARS-WG) that uses more flexible semi-empirical approach compared to the Markov chain approach that uses a simple standard distribution to generate series of wet and dry day. In LARS-WG, daily Tmax and Tmin are modeled separately as stochastic processes with daily means and standard deviation conditioned on the wet or dry status of the day (Semenov and Brooks, 1999). The seasonal cycles of means and standard deviations are modeled by finite Fourier series of order 3 which is constructed using observed mean values, sine and cosine curve and phase angle for each month. LARS-WG also uses autocorrelation values for Tmin and Tmax derived from observed weather data to model the temperature. LARS-WG is available to the broader climate change impact study community via Environment Canada web site (http://www.cccsn.ec.gc.ca/index.php?page=lars-wg).

Monthly statistical parameters of climates observed at the Coleman climate station are extracted using LARS-WG, and a new set of daily climates for the reference period 1965 -1997 are generated. These generated climates are compared with the observed climates at Coleman station to evaluate the performance of LARS-WG. Once reference climates are generated and validated, nine sets (for three different scenarios: A1B, A2 and B1, and for three different time periods: 2020s, 2050s and 2080s) of future periods daily climates are generated disaggregating the future monthly climate means estimated for Coleman station. Although observed daily climates are available for reference period, we use stochastically generated climates to provide input to the hydrological model to simulate the reference period streamflow. This makes the reference and future periods streamflows comparable because they are generated with the same methods, but reflect the statistical properties of the climate periods.

Hydrological model calibration, application and parameters uncertainty

HBV-EC

A common conceptual hydrological model, HBV-EC is used to study the hydrological impacts of climate change. HBV-EC is a version of the conceptual HBV model (Bergstrom and Forsman, 1973; Lindström et al., 1997) that simulates daily/hourly discharge using daily/hourly precipitation and temperature and monthly estimates of evapotranspiration as input. The model is based on the concept of grouped response units (GRUs) that groups DEM/GIS grid cells having similar elevation, aspect, slope and land cover. HBV-EC uses elevation bands subdivided into different land types (open, forest, glacier and water), slopes and aspects. Lateral climate gradients in HBV-EC are represented by subdividing the basin into different climate zones; each of which is associated with a climate station and a unique parameters set (Jost et al., 2012). The model consists of three main modules: 1) a snow module that simulates snow accumulation and a degree-day snowmelt approach; 2) a soil module that simulates groundwater recharge and actual evaporation as functions of soil moisture; and 3) a runoff transfer module that consists of one upper nonlinear reservoir representing fast and one lower linear reservoir representing slow responses to delay the runoff in time. Detailed descriptions of HBV-EC are given by Hamilton et.al (Hamilton et al., 2000). HBV-EC is an open source, available at modeling framework 'Green Kenue' (http://www.nrc-cnrc.gc.ca/eng/solutions/advisory/green_kenue/download_green_kenue.html) developed by National Research Council Canada in collaboration with Environment Canada.

Hydrological Model Calibration

HBV-EC model is driven by the thirty two years (1965-1997) climates recorded at the Coleman climate station to simulate the streamflow which is compared with observed flow at Frank. The watershed is divided into five different elevation zones which are further divided into different land use types, slope and aspects. Temperature and precipitation lapse rates within the watershed are calculated using the climateWNA generated monthly climate data. The model was calibrated using the optimization algorithm Genoud (written in the rgenoud R application (Mebane and Sekhon, 2011)) that combines evolutionally algorithm methods with steepest gradient descent algorithm (Jost et al., 2012) to maximize the Nash-Sutcliffe efficiency (NSE) (Nash and Sutcliffe, 1970) of the streamflow.

Application

The calibrated model is then driven by the LARS-WG generated daily climates to simulate the streamflows for reference and future periods. Reference period model simulated streamflow is compared with observed flow to determine how well the LARS-WG generated climate can represent the properties of the observed streamflow. Simulated streamflows for the reference and future periods are compared to assess the climate change impacts.

Parameter uncertainty

In HBV-EC model parameters can be interdependent, and different parameter sets can produce good results (high NSE) for one period but not for another (Beven, 2000; Seibert et al., 2010; Steele-Dunne et al., 2008). To address this problem of parameter uncertainty, a Monte Carlo technique was employed and 100 most efficient model parameters sets that results in NSE values higher than the obtained from the Genoud, minus a threshold are selected. These 100

parameters sets are used with HBV-EC to provide a range of model results to helps to understand the model sensitivity to the parameters uncertainty.

Forest change

A change detection modeling technique suggested by Seibert and McDonnel (2010) and Seibert et al. (2010) is used to assess the impacts of forest change on the streamflow. Seibert et al. (2010) used similar hydrological model to quantify the impacts on streamflow after forest removal from a watershed due to wildfire. We remove forest from the watershed and run HBV-EC for reference and future periods to understand how removal of forest in reference and future periods would impact the streamflow.

2.3 Results

2.3.1 Estimates of future monthly climate means

Relative changes in watershed averaged monthly climate means observed in GCM outputs for nine different future scenarios are in Table 2.1. GCM projections showed an increase in precipitation during winter (December, January and February) and decrease in precipitation during summer (June, July and August) for our watershed. Projections for spring (March, April and May) and fall (September, October and November) were mixed. There was consistent increase in mean temperature for all seasons of the year (Table 2.1).

Table 2.1 Relative changes in watershed averaged mean monthly GCM projections of precipitation and air temperature for A1B, A2 and B1 scenarios for 2020s, 2050s and 2080s time periods.

Time period	Scenario	Jan	Feb	Mar	Apr	May	Jun	Jul	Aug	Sep	Oct	Nov	Dec	Annual	Annual mean
Percentage change in mean monthly precipitation, ΔP															
2011-	A1B	2.6	4.1	-4.3	3.9	-7.3	-5.0	-2.4	-2.8	3.2	-2.7	-7.9	3.6	-1.6	-1.708
2040	A2	3.1	3.8	-4.5	3.5	-7.3	-5.2	-2.3	-3.1	2.7	-2.6	-7.7	3.6	-1.6	
("2020s")	B1	2.3	3.6	-4.2	3.9	-7.8	-5.6	-2.6	-3.6	2.8	-3.5	-7.7	3.4	-1.9	
2041-	A1B	4.2	4.7	-2.9	4.9	-6.6	-4.6	-1.6	-1.8	4.3	-1.9	-6.7	4.8	-0.6	-0.980
2070	A2	3.7	4.4	-3.0	5.0	-6.1	-4.5	-1.3	-1.5	4.3	-1.9	-7.0	4.5	-0.6	
("2050s")	B1	3.7	2.6	-3.6	3.8	-7.9	-5.2	-2.0	-3.2	3.0	-3.4	-7.5	3.1	-1.7	
2071-	A1B	5.3	4.4	-1.9	4.6	-6.0	-3.8	-0.6	-1.0	4.9	-1.3	-6.4	6.3	0.04	0.002
2000	A2	6.7	6.8	-1.2	6.1	-5.0	-3.1	0.5	-0.1	6.1	-0.6	-6.0	6.8	1.1	
("2080s")	B1	3.9	4.5	-2.7	4.5	-6.9	-5.2	-2.0	-2.5	3.5	-3.2	-7.0	4.2	-1.1	
Change in mean monthly air Temperature, $(\Delta T_{max} + \Delta T_{min})/2$															
2011-	A1b	1.6	3.1	0.9	0.7	1.0	1.6	1.5	1.7	1.5	0.8	0.9	0.7	1.3	1.4
2040	A2	2.0	2.8	0.6	0.4	1.2	1.7	1.8	1.8	1.1	0.9	1.0	0.8	1.3	
("2020s")	B1	1.7	3.6	1.5	1.0	1.1	1.3	1.6	1.3	1.2	1.2	1.1	1.1	1.5	
2041-	A1B	3.1	3.6	2.2	1.2	1.7	2.0	2.5	2.7	2.2	1.7	2.0	1.8	2.2	2.1
2070	A2	2.6	3.4	1.8	1.6	2.2	2.0	2.4	3.0	2.6	1.9	1.6	1.6	2.2	
("2050s")	B1	3.0	2.7	2.0	0.9	0.9	2.4	2.5	1.9	1.9	1.3	1.4	0.8	1.8	
2071-	A1B	3.8	3.2	2.9	1.0	2.4	3.1	3.7	3.5	2.8	2.1	2.4	3.0	2.8	3.0
2000	A2	5.2	5.3	3.3	2.2	3.4	3.7	4.5	4.6	4.0	2.7	2.8	3.6	3.8	
("2080s")	B1	3.8	4.3	3.0	1.6	2.1	2.1	2.4	2.7	1.8	1.3	1.8	1.8	2.4	

Future monthly climate means (precipitation, T_{max} and T_{min}) at the Coleman climate station for the nine scenarios along with the reference period observed climate aggregated to monthly scale are presented in Figure 2.2. Disaggregation of these provides climate inputs to the hydrological model to simulate reference and future periods streamflows. Figure 2.2 shows higher precipitation during winter and lower precipitation during summer for future periods in comparison to reference period. However, the increase or decrease in future periods precipitation compared to reference period was less than 10% for any seasons. T_{max} and T_{min} for future periods are higher for all seasons.

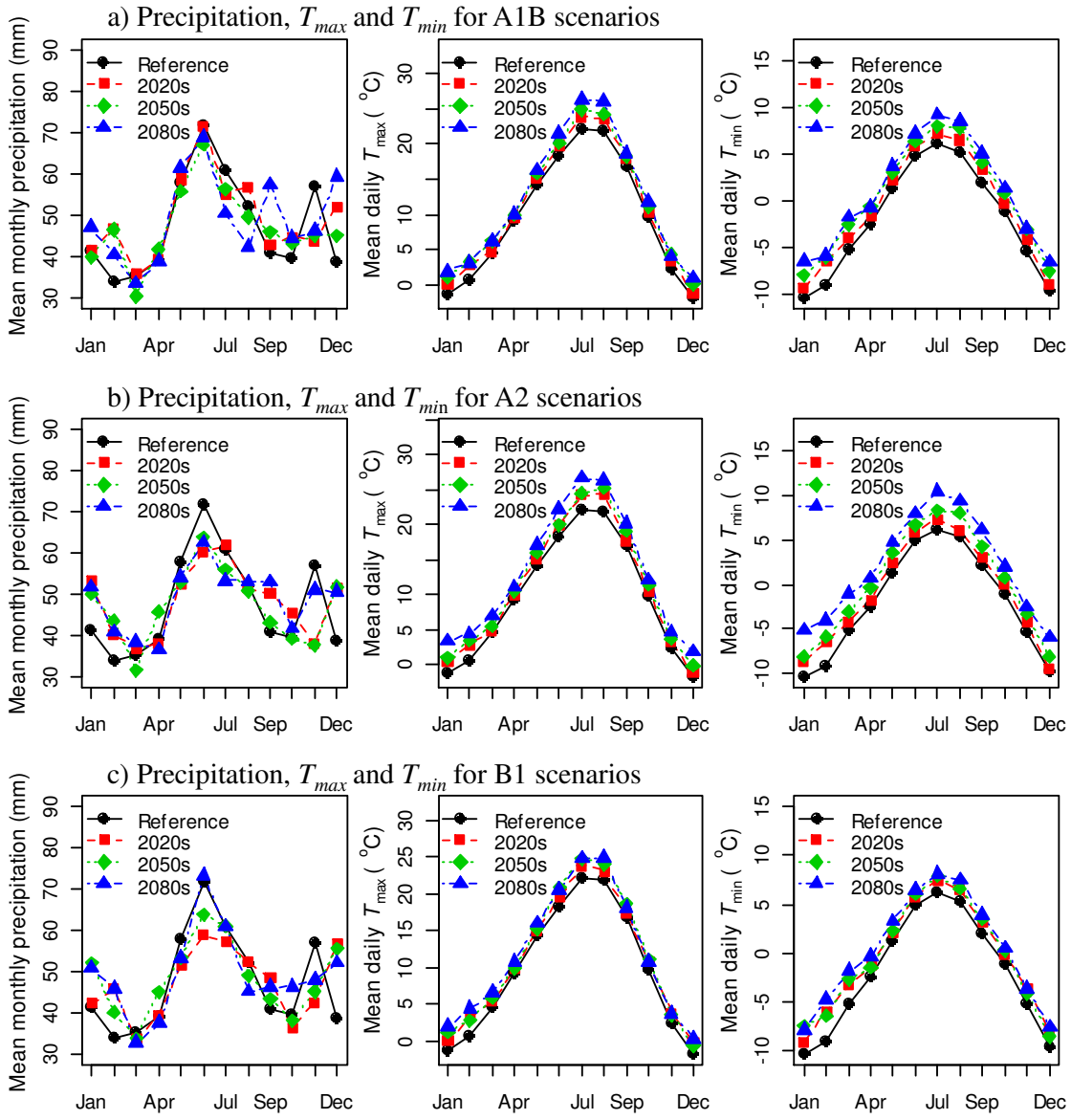

Figure 2.2 Reference (observed) period daily climates aggregated to monthly scale and nine sets of future monthly climate means (precipitation, Tmax and Tmin) estimated for climate station, Coleman.

2.3.2 Disaggregation

LARS-WG model performance was evaluated by comparing the observed and LARS-WG generated means and variances for monthly precipitation by using *t*- and *f*-test, respectively and means of daily T_{max} and T_{min} by using the *t*-test (Table 2). LARS-WG reproduced hundred percent (for all twelve months) monthly means for precipitation well giving p-values higher

than 0.05 suggesting not significant difference in means at the 95% confidence level as shown in Table 2.2. However, only 75% of monthly variances for precipitation were reproduced by the model (4 out of 12 p-values for the *f*-test are less than 0.05). LARS-WG produced mixed results for T_{min} and T_{max}. The *t*-tests for the T_{min} were significant for 4 months out of 12 (4 out of 12 p-values for the *t*-test are less than 0.05) and the *t*-tests for the T_{max} were significant for 2 months out of 12 months (2 out of 12 p-values for the *t*-test are less than 0.05). Comparison of LARS-WG simulated mean monthly precipitation and monthly mean values of daily T_{max} and T_{min} with observed climates are presented in the Figure 2.3.

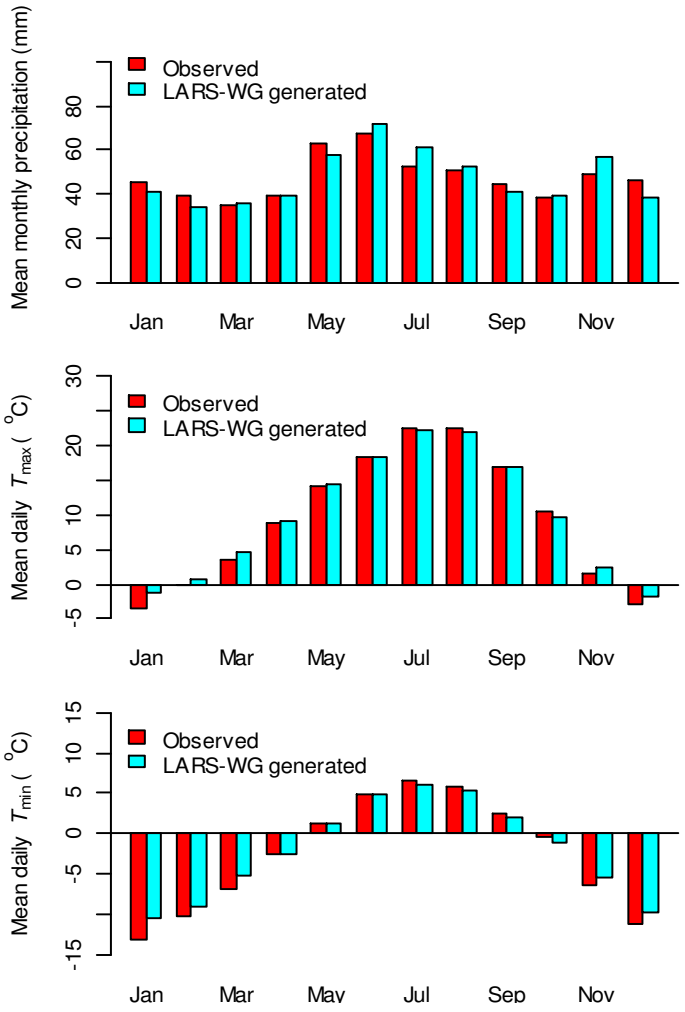

Figure 2.3 Observed and LARS-WG generated monthly values of precipitation, T_{max} and T_{min}.

Table 2.2 Comparison of monthly statistics of daily precipitation, Tmax and Tmin observed at Coleman station during the period from 1965 to 1997 with synthetic data generated by LARS-WG. P-values calculated by the t-test and F-test for the monthly means and variances are shown. A probability of 0.05 or lower indicates a departure from the observations that is significant at the 5% level.

	Jan	Feb	Mar	Apr	May	Jun	Jul	Aug	Sep	Oct	Nov	Dec
Precipitation												
Observed mean	45.10	39.13	34.98	39.03	63.24	67.58	52.56	50.98	44.42	38.19	48.70	45.91
Observed standard deviation	31.80	31.59	21.59	17.63	29.39	26.19	40.22	39.99	26.67	24.34	33.15	30.23
Generated mean	41.36	33.85	35.42	39.34	57.96	71.61	60.82	52.11	41.01	39.62	56.99	38.60
Generated standard deviation	21.67	17.00	20.24	17.64	25.49	25.81	23.65	20.02	22.19	21.19	32.38	22.44
P-values for T-test	0.583	0.406	0.933	0.943	0.442	0.535	0.319	0.887	0.577	0.803	0.315	0.276
P-values for F-test	0.036	0.001	0.720	0.995	0.431	0.936	0.03	0.03	0.309	0.445	0.896	0.102
T_{min}												
Observed mean	-13.05	-10.09	-6.87	-2.63	1.35	4.95	6.61	5.86	2.46	-0.46	-6.39	-11.15
Observed standard deviation	4.76	4.06	2.93	1.69	0.95	1.16	1.02	1.20	1.38	1.58	3.16	4.32
Generated mean	-10.41	-9.10	-5.21	-2.51	1.32	4.93	6.15	5.33	2.07	-1.13	-5.30	-9.67
Generated standard deviation	1.82	1.72	1.32	0.83	0.65	0.71	0.49	0.63	0.97	1.21	1.44	1.73
P-values for T-test	0.005	0.208	0.005	0.734	0.914	0.944	0.024	0.031	0.188	0.062	0.080	0.078
T_{max}												
Observed mean	-3.51	-0.02	3.55	8.91	14.22	18.38	22.37	22.36	16.90	10.41	1.66	-2.83
Observed standard deviation	4.07	3.14	2.85	2.21	1.85	1.84	2.14	2.55	3.43	2.23	2.91	3.34
Generated mean	-1.25	0.64	4.64	9.21	14.24	18.30	22.12	21.84	16.85	9.66	2.33	-1.86
Generated standard deviation	1.38	1.13	0.83	1.09	1.22	0.93	1.08	1.04	1.38	1.30	1.10	1.19
P-values for T-test	0.006	0.263	0.052	0.499	0.957	0.826	0.558	0.282	0.935	0.106	0.227	0.128

2.3.3 HBV-EC Calibration

Figure 2.4 compares the observed daily streamflow at watershed outlet, Crowsnest at Frank with HBV-EC simulated values for the calibration period 1965–1997. Both peak and low flows were simulated reasonably well except few higher peaks were underestimated by the model (Figure 2.4). NSE of 0.82 was obtained during this calibration period. Differences in mean monthly streamflow between the observed and simulated values range from -15 to 50%. The large difference observed was during the month of February. Though the difference was large in percentage, in terms of magnitude the difference was very small, about 5 mm. Maximum of 12 mm difference was observed in the month of June. Differences between the observed and simulated annual flows range from -25% to 40%. The large differences (>|15%|) observed were during the years 1968, 1969, 1973, 1974,1988, 1991 and 1994. In other years the differences were less than |15%|. While there were discrepancies in the simulated versus observed mean monthly and annual flows, the negative and positive errors offset each other giving only 6% (about 25 mm) difference in mean annual flow between the observed and simulated values.

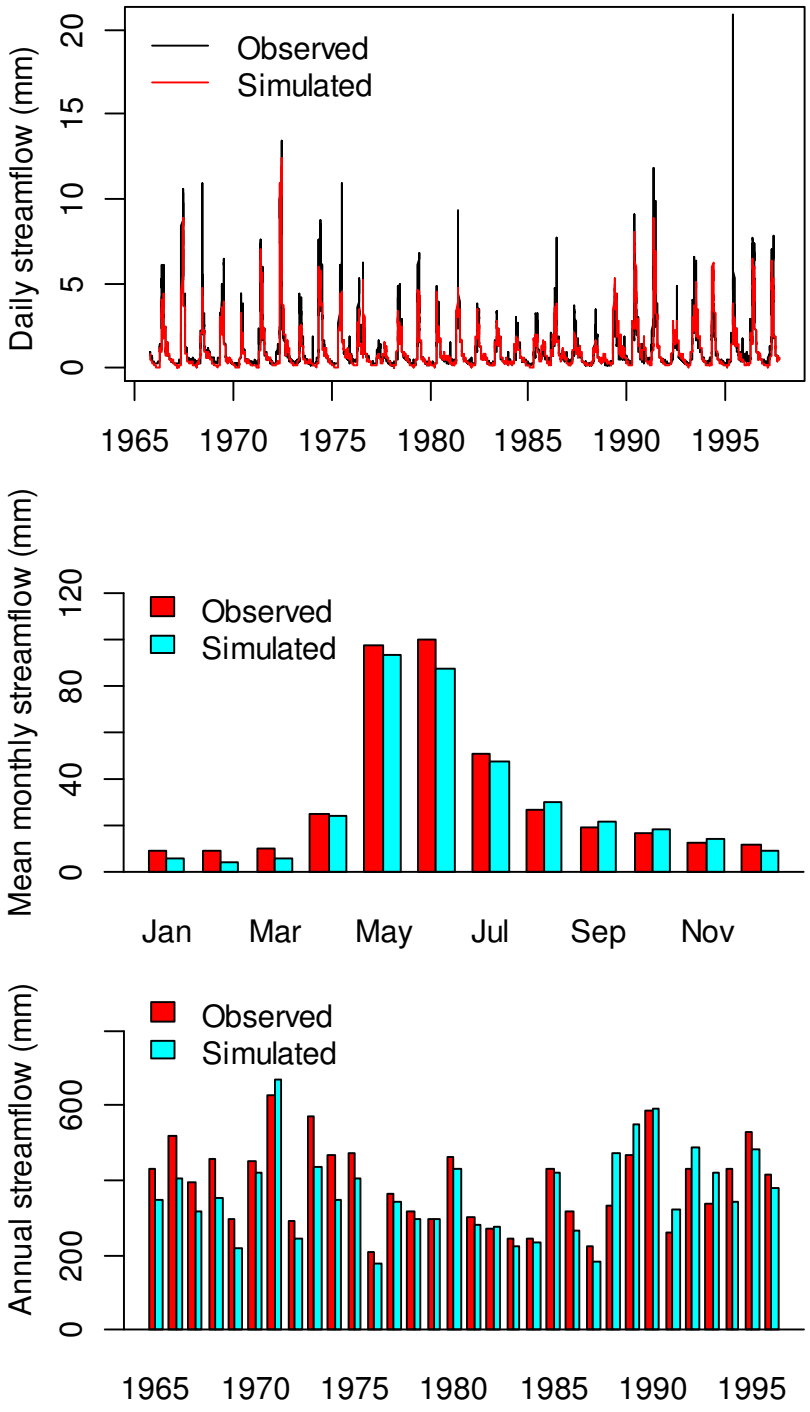

Figure 2.4 Observed and HBV-EC simulated daily, monthly and annual streamflows during the calibration period from 1965 to 1997. HBV-EC is driven by the daily climates observed at Coleman station.

2.3.4 HBV-EC Application

Figure 2.5 compares the model simulated streamflow (daily, monthly and annual) with the observed streamflow values at study watershed outlet, Crowsnest at Frank. Input to the HBV-EC in this case is LARS-WG generated daily realizations. Daily, monthly and annual comparisons (Figure 2.5) show that the streamflow simulated are realistic and close to the observed values as in Figure 2.4. However, the NSE was not that great. This is somewhat expected given the generated weather data captures the stats but not the actual amounts.

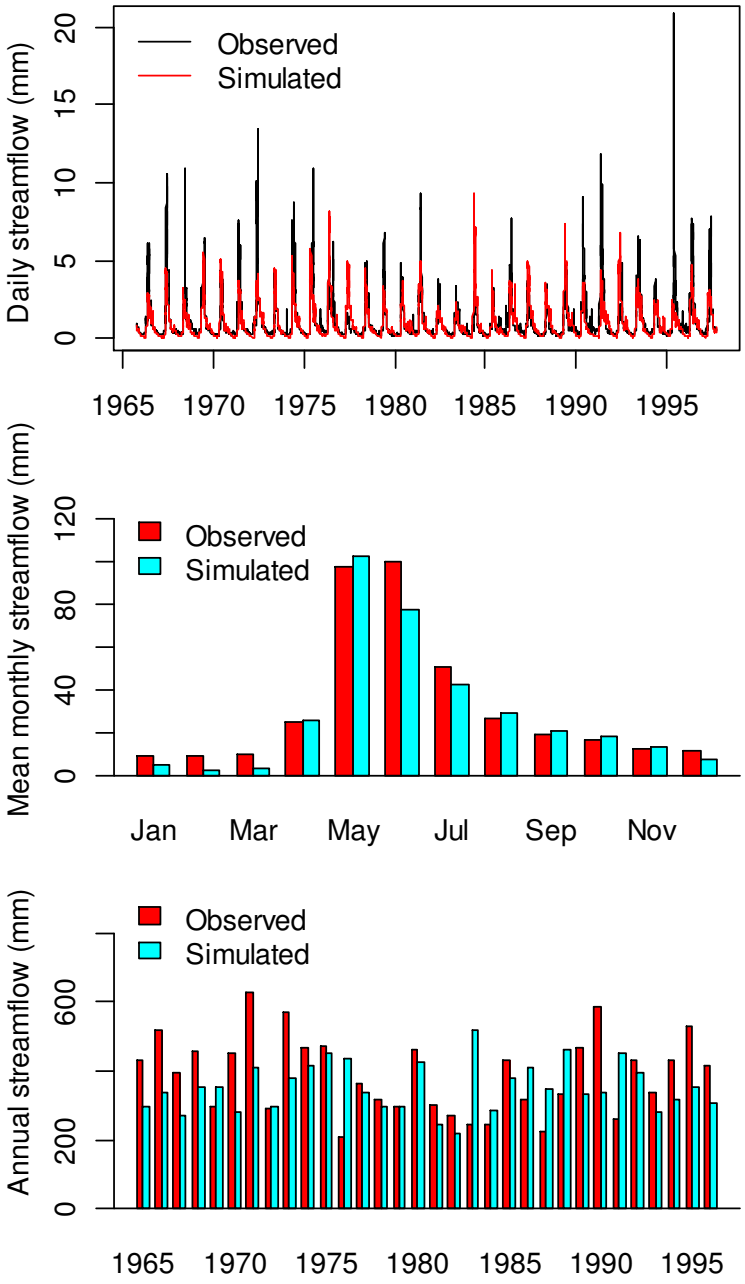

Figure 2.5 Same as figure 4, but in this case HBV-EC is driven by the LARS-WG generated daily climates.

Figure 2.6 compares the HBV-EC simulated streamflows at watershed outlet, Crowsnest at Frank for reference and nine future periods. Mean monthly hydrographs of all future simulations (Figure 2.6) showed early initiation of peaks resulting in the seasonal shift, a shift toward higher spring (March, April) flows and a corresponding decrease in summer (June and July) flows associated with the shift in the spring flows compared to reference periods hydrographs. Future simulations also showed an increase in the winter low flows. Winter low flows increased up to 200% (9.3 mm) in February while summer high flows decreased up to 63% (31.2 mm) in June in A2 scenario in 2080s time period. Fall (September, October and November) flows were affected less and remained almost same for all future periods. Despite the variations in the mean monthly flows, mean annual flows for the reference and future periods were quite similar (Figure 2.6). Maximum increase in mean annual flow was found to be projected about 9% in 2080s for A2 scenario while maximum decrease was found to be projected about 6% in 2050s for A1B scenario.

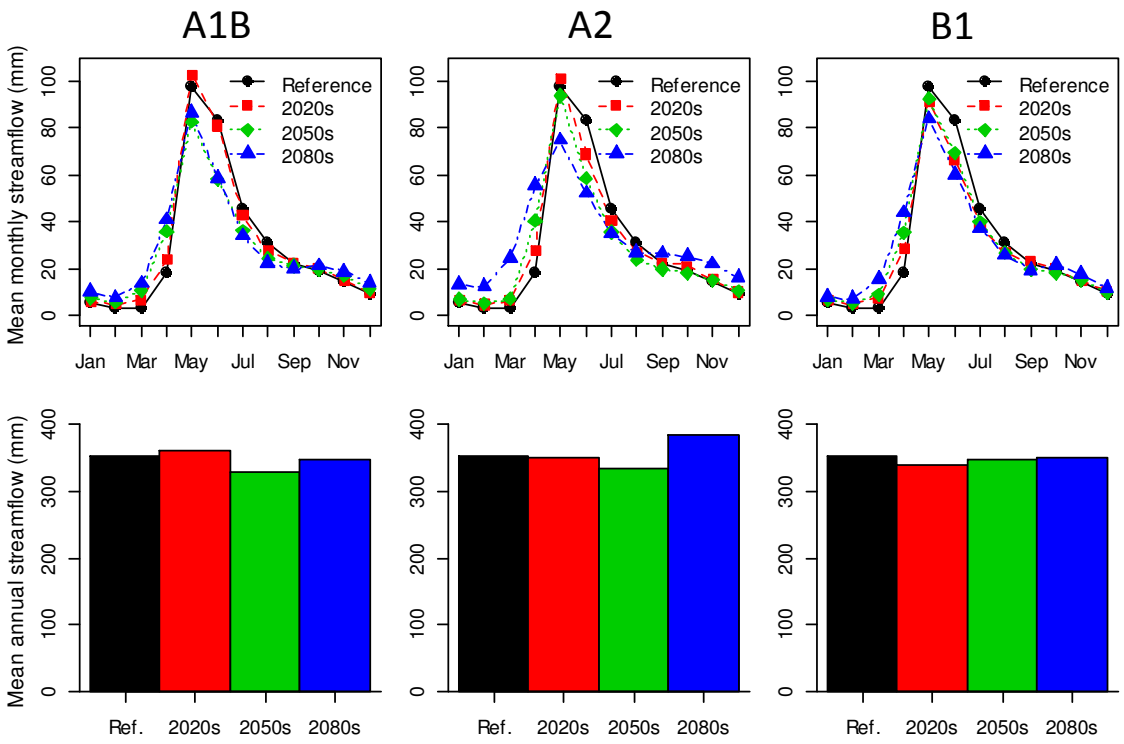

Figure 2.6 HBV-EC simulated mean monthly and mean annual streamflows for the reference and nine future periods (for three different scenarios: A1B, A2 and B1and for three different time periods: 2020s, 2050s and 2080s) at the watershed outlet at Crowsnest at Frank.

Reference and future periods mean monthly snow water equivalent (SWE) and mean monthly evapotranspiration for the study watershed are presented in Figure 2.7. SWE values decreased in all future simulations. Evapotranspiration increased in spring and decreased in summer. Despite increase in temperature throughout the year, decrease in evapotranspiration during the summer indicates water deficit and unavailable for evapotranspiration during the summer.

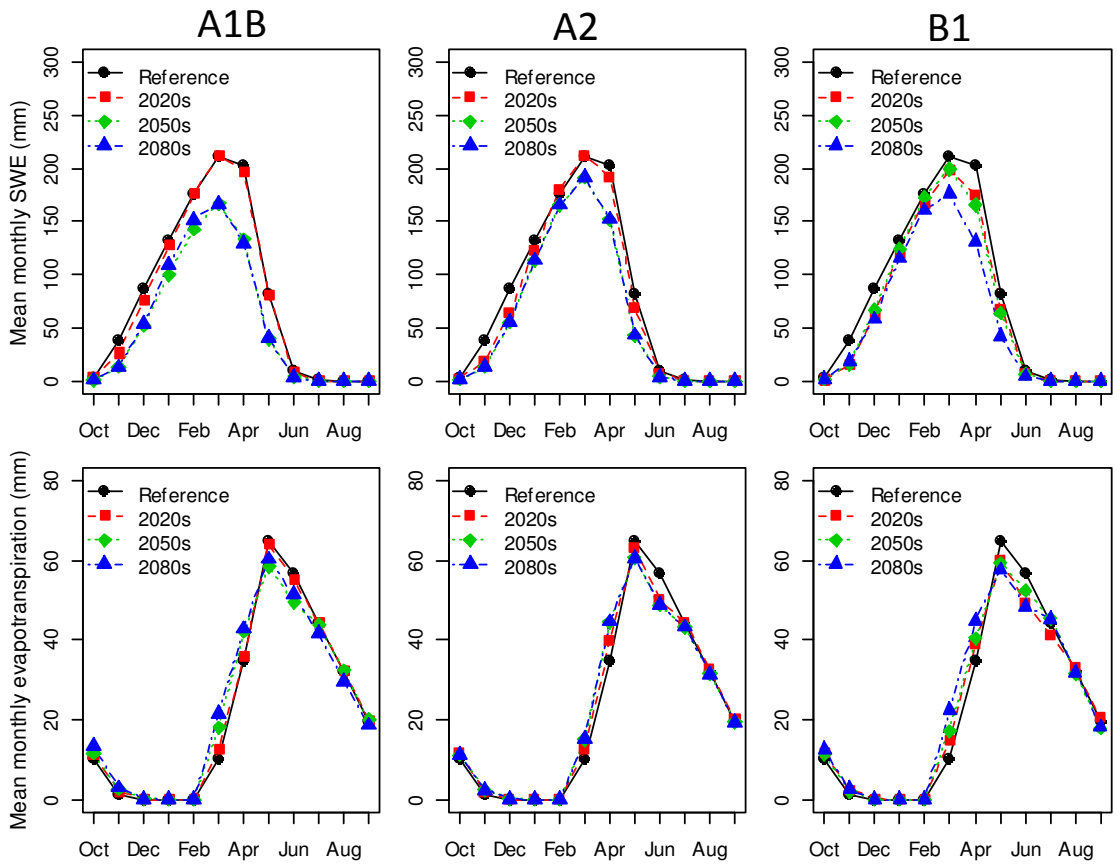

Figure 2.7 HBV-EC simulated watershed averaged mean monthly snow water equivalent (SWE) and mean monthly evapotranspiration for the reference and future periods.

2.3.5 Parameter Uncertainty

Relative changes in mean monthly streamflows in different future periods compared to reference period were calculated from the HBV-EC ensemble simulations (Figure 2.8). Ensemble spread was found to be higher in spring and summer than in winter and fall in all future scenarios indicating higher parameter uncertainty impacts on spring and summer flows than on winter and fall flow. Single simulation showed maximum of about 31.2 mm of streamflow reduction during summer while the ensemble showed up to 80 mm reduction in streamflow in summer. Ensemble mean showed about 46 mm reduction in summer flow which is about 1.5 times higher than that the single simulation predicted.

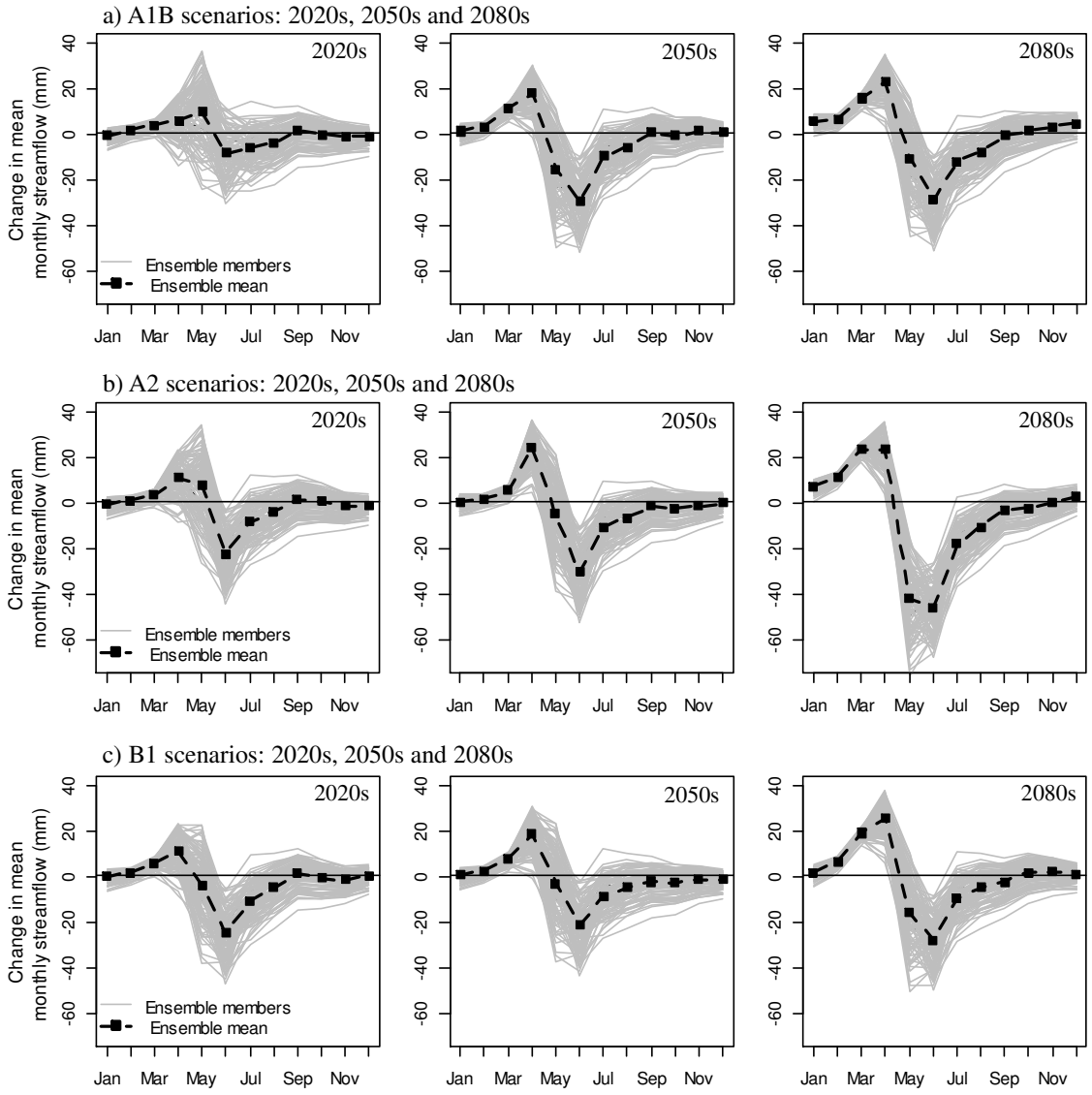

Figure 2.8 Ensemble of relative changes in mean monthly streamflows in different future periods compared to reference period streamflow, and mean of the ensemble.

2.3.6 Forest Change

Ensemble streamflows were generated using best 100 parameter sets to assess the forest change impacts. Only one scenario: 2080s with A2 climate scenario, was selected to study the combined climate and forest change impacts on streamflow as climate change impact to represent the possible worst case scenario. Figure 2.9a, 2.9b and 2.9c show relative changes in mean monthly streamflow (ensemble and mean) due to forest removal (Figure 2.9a), due to

climate change (Figure 2.9b), and due to combined forest removal and climate change (Figure 2.9c). Mean values of these ensembles are also compared in Figure 2.9d. Removal of forest from the watershed increased streamflow in early spring, late summer and early fall, and reduced streamflow in late spring and early summer. The mean ensemble (Figure 2.9d) shows a higher increase in winter flow due to the combined forest removal and climate change impact compared to individual impact produced by forest removal or climate change. However, the combined impact on the summer flow was less compared to the climate change impact, suggesting that the forest had a roll in the summer evapotranspiration and streamflow.

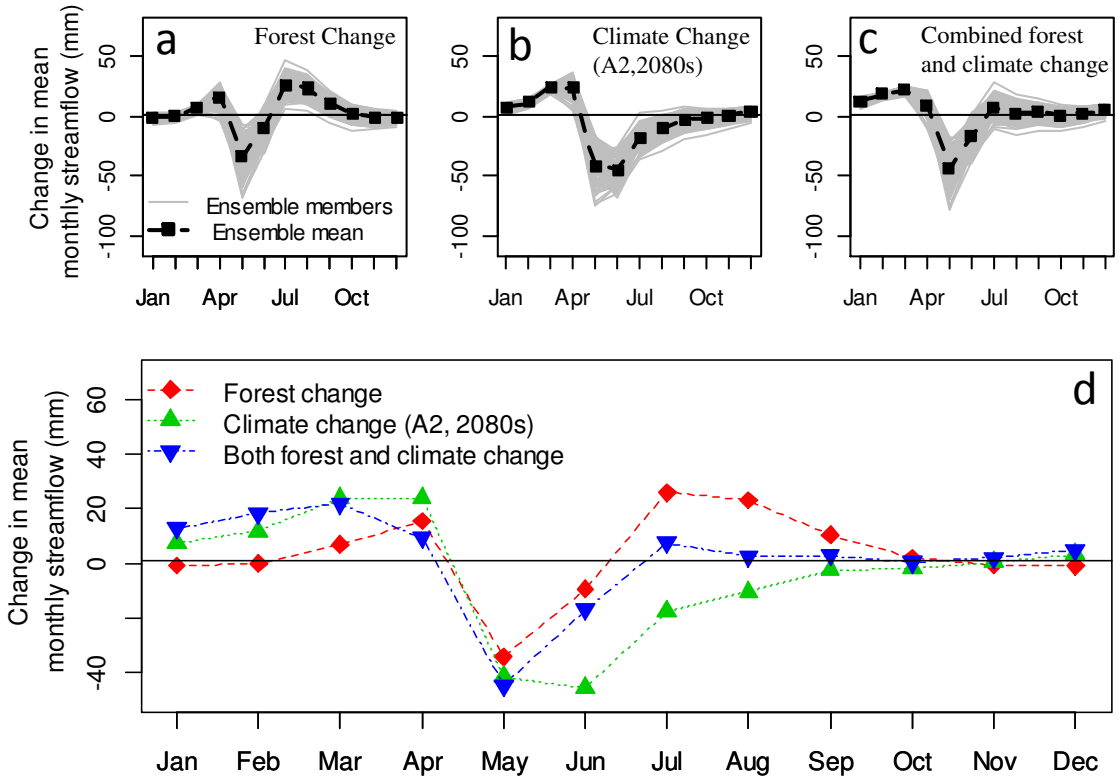

Figure 2.9 Ensemble and mean values of relative changes in mean monthly streamflows: a) due to forest removal b) due to climate change in 2080s in A2 scenario and c) due to combined forest removal and climate change in 2080s in A2 scenario. Figure 9d shows the ensemble mean to compare the relative changes in mean monthly streamflows due to forest removal, due to climate change in 2080s in A2 scenario and due to combined forest removal and climate change in 2080s in A2 scenario.

2.4 Discussion

This study uses GCM outputs downscaled using ClimateWNA model with two other models: LARS-WG and HBV-EC to assess the impacts of climate and forest changes on streamflow. These types of studies inherently have large sources of uncertainty in predictions and are used to inform trends rather provide predictive results. Inclusion of uncertainty estimates in GCM simulations, ClimateWNA downscaling or and LARS- WG disaggregation may provide the robust assessment of the impacts of climate change on water resource systems. However, analyses of uncertainty in the climate simulations and downscaling are beyond the scope of this study. Uncertainty in the LARS-WG disaggregation and hydrological modeling are analyzed and partly taken into account.

LARS-WG reproduced monthly means and variances for the precipitation very well; it demonstrated relatively poor performance, especially, in reproducing the monthly variances of T_{max} and T_{min}. Mixed results were obtained in reproducing means of T_{max} and T_{min}. The possible source of error could be the use of many pre-set values in the model. While estimating an average daily standard deviation for T_{max} and T_{min}, LARS-WG normalises the temperature residuals using constant auto-correlations and cross-correlations between the temperature residuals through the year. Those constant values are site specific and might be different for our climate. *Semenov and Brooks* (1999) recommend site specific testing and validation of model before the generated data are used in an application for a sensitive application, where more accuracy is required for each variable, for example, in a study of extreme weather event. For this study LARS-WG can be implemented without any changes in the model. Although the model did not reproduce the variances very well, it reproduced the average behaviour of observed data and so the performance for mean precipitation and temperature was good.

The hydrological model used in this study is a conceptual model and does not represent many physical processes. However, the choice was governed by the availability of data. Observed climate and other data available for model input and verification were limited. Although there are some climate stations at higher elevations, their records were short and seasonal. More detailed models may represent the physical processes thoroughly, but use of these models under such conditions may cause problems of over-parameterization, parameter estimation and validation limitations.

HBV-EC reasonably captured the reference period daily streamflow with NSE 0.82 as well as monthly and annual flow very well. Streamflow simulated using LARS-WG generated climates also matched the daily, monthly and annual observed streamflow reasonably, though the NSE value was low and model error was large. However, the error that LARS-WG produced is inherent and would be consistent in both reference and future period simulations and would not affect much in the evaluation of climate and forest change impacts.

Hydrological model in this study was calibrated against the streamflow measurements only. It would have been better if we were able to calibrate the model against other measurements, i.e., SWE, soil moisture content or evapotranspiration before the model being used to simulate future streamflows. But the limited data did not afford such luxury to validate model against other measurements.

Comparison of HBV-EC simulated flows for the reference and future periods in climate change studies suggest an amplification of the seasonal cycle with increased winter precipitation leading to a rise in winter (DJF) stream flow. Increase in streamflow during the winter could

have been caused by the partly replacement of snowfall by rainfall due to the increased in temperature during the season when potential evapotranspiration rates are low (Forbes et al., 2011). Combination of increased temperature and decreased precipitation resulted in reduction in May and summer (JJA) streamflow. Previous climate change studies carried out in similar regions in Canada (e.g. Dibike and Coulibaly, 2005; Forbes et al., 2011; Kienzle et al., 2012) have also found streamflows increased in winter and spring, and decreased in summer. These changes (increased or decreased in streamflow) we found were relatively higher for A2 climate scenario, which is reflective of largest changes to climate when compared to other two scenarios.

The model parameter uncertainty analysis showed streamflow predictions to vary considerably. This higher spread observed in ensemble simulations in summer indicates a higher risk of lower summer flows than was predicted by the single simulation. Combined climate and forest change impact compounded the effect increasing winter flow; however, it did not reduce the summer flow much. The higher winter or early spring flow in both reference and future periods observed after removal of forest may be caused by the quicker snowmelt when forest was removed. Usually the removal of forest results in increased summer flow due to the less evapotranspiration during the summer or fall. But in our case the model doesn't distinguish the difference in evapotranspiration based on the presence or absence of the forest, thus the less reduction in the simulation of summer flow when forest was removed is possibility due to the higher soil recharge during the winter and increased soil moisture release during the summer.

2.5 Conclusion

A watershed in the eastern slopes of the Southern Alberta Rocky Mountains was modeled to investigate the potential impacts of climate and forest changes on its hydrology using a simple conceptual hydrological model, HBV-EC. Monthly climate data downscaled to 1x1 km grids are disaggregated to daily realizations using stochastic weather generator, LARS-WG. These realizations provided the inputs to the HBV-EC to simulate reference and future scenarios streamflows that are compared to assess the climate and forest change impacts. Climate change impacts are mainly observed in the seasonality of streamflow: higher winter flows and lower summer flows. These are mainly caused by the increase in temperature as there was not much difference in precipitation between reference and future periods. Summer flows were found to be more vulnerable and the consequences are less availability of summer water in the river which is already stressed due to higher demand than the supply. The use of an ensemble of parameter sets in this study allowed us to examine the impact of parameter uncertainty in the streamflow simulations. However, uncertainties exist in model simulations of many hydrologic components (i.e., soil moisture, base flow, snow accumulation and ablation, evapotranspiration etc.) that are not validated in this study. Poor representations of these may largely affect the model results in the simulations of future streamflows for climate change studies.

2.6 Acknowledgements

This research was supported by Alberta Innovates, Bio Solutions. We are especially grateful to Mike Wagner, Chris Williams and Amanda Martens for technical assistance.